

Anomalous diffusion in a dynamical optical lattice

Wei Zheng and Nigel R. Cooper

T.C.M. Group, Cavendish Laboratory, University of Cambridge, J. J. Thomson Avenue, Cambridge CB3 0HE, United Kingdom



(Received 12 September 2017; published 5 February 2018)

Motivated by experimental progress in strongly coupled atom-photon systems in optical cavities, we study theoretically the quantum dynamics of atoms coupled to a one-dimensional dynamical optical lattice. The dynamical lattice is chosen to have a period that is incommensurate with that of an underlying static lattice, leading to a dynamical version of the Aubry-André model which can cause localization of single-particle wave functions. We show that atomic wave packets in this dynamical lattice generically spread via anomalous diffusion, which can be tuned between superdiffusive and subdiffusive regimes. This anomalous diffusion arises from an interplay between Anderson localization and quantum fluctuations of the cavity field.

DOI: [10.1103/PhysRevA.97.021601](https://doi.org/10.1103/PhysRevA.97.021601)

One of the most interesting directions of research in coherent quantum systems concerns the collective dynamics of coupled atom-photon ensembles. Such situations arise for cold atomic gases in optical cavities [1] or waveguides [2,3], where strong coupling between the atomic motion and a photon field can be achieved. Coupling cold atoms even to a single cavity mode can dramatically change the steady state of the atomic gas [4–25] and lead to interesting nonequilibrium dynamics [26–36].

A transversely pumped Bose-Einstein condensate in a single-mode cavity can undergo a phase transition into a self-organized “superradiant” state in which the cavity mode becomes highly occupied and generates a cavity-induced superlattice potential on the atoms. For current experiments [8,9] this dynamical cavity-induced superlattice is commensurate with an underlying static optical lattice, therefore giving rise to a supersolid phase with extended Bloch waves. However, one can readily envisage situations in which the cavity-induced superlattice is incommensurate with the underlying static lattice. This leads to the interesting possibility that the cavity-induced superlattice leads to localization of the single-particle states. Indeed, several theoretical works have studied the steady state of cold atoms in such settings [37–39] and have found a self-organized localization-delocalization transition within a mean-field approximation.

In this Rapid Communication, we show that the motion of atoms in a cavity-induced incommensurate lattice is qualitatively affected by the quantum fluctuations of the cavity field, leading to long-time behavior that is not captured by mean-field theories. Specifically, we show that the atomic motion exhibits anomalous diffusion in which the width of the wave-packet σ grows with time as $\sigma \sim t^\gamma$ with $0 < \gamma < 1$. Anomalous diffusion exists widely in both classical and quantum systems. In classical random walks, anomalous diffusion is mostly associated with the failure of the central limit theorem and the presence of long-tailed distributions [40–42]. On the other hand, in closed quantum systems, anomalous diffusion is typically connected to the multifractal nature of eigenstates [43,44]. Nonlinearity associated with many-body interactions can also weakly destroy Anderson

localization and lead to anomalous diffusion [45–51]. In our model, anomalous diffusion arises in a very distinct way: via the coupling of a quantum particle to a single quantum oscillator (the cavity mode) subjected to simple Markovian damping. We show that the dynamics of the resulting *open* quantum system can be viewed as a form of Lévy walk with rests [52–55]. This explanation relies both on quantum fluctuations of the cavity field and on Anderson localization in the incommensurate potential and so is an inherently quantum phenomenon. Owing to the central role played by the cavity mode, we predict that evidence of this anomalous transport can be found in long-tailed distributions of photon correlations in the cavity field.

Model. We consider spinless atoms trapped by an optical lattice in a high- Q cavity (Fig. 1), both aligned along the x direction [56]. Two counterpropagating pump lasers are shone on the atom cloud from the z direction. Denoting the cavity field operator by \hat{a} , the net potential on the atoms is $V = A_0 \cos^2(k_0 x) + B_0 \hat{a}^\dagger \hat{a} \cos^2(k_c x + \phi) + C_0 (\hat{a} + \hat{a}^\dagger) \cos(k_p z) \cos(k_c x + \phi) + V_\perp(y, z)$. Here A_0 is proportional to the optical lattice intensity, B_0 is the cavity-atom coupling strength (ϕ controls the relative positions of the optical lattice and the cavity mode), and C_0 is the pump-cavity coupling proportional to the amplitude of the pump laser. We consider the transverse confinement to be sufficiently large that the transverse motion is frozen out. For deep enough lattices, we obtain a one-dimensional tight-binding model as [9,57]

$$H = \Delta \hat{a}^\dagger \hat{a} - J \sum_{j=1}^L (\hat{c}_{j+1}^\dagger \hat{c}_j + \text{H.c.}) + \lambda (\hat{a} + \hat{a}^\dagger) \sum_{j=1}^L u_j \hat{c}_j^\dagger \hat{c}_j + U \hat{a}^\dagger \hat{a} \sum_{j=1}^L u_j^2 \hat{c}_j^\dagger \hat{c}_j, \quad (1)$$

where $\hat{c}_j^{(\dagger)}$'s are the atomic field operators on lattice site j ; $\Delta = \omega_c - \omega_p$ is the detuning of the cavity mode; $u_j = \cos(2\pi\beta j + \phi)$, $\beta = k_c/2k_0$; U and λ are the projections of B_0 and C_0 onto the Wannier functions. We have ignored interactions between atoms as can be realized by a Feshbach

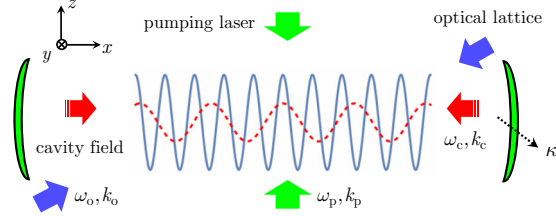


FIG. 1. Schematic of the experimental setup. Atoms in an optical lattice and a standing-wave cavity are driven by a transverse laser. The frequency ω_p of the pump laser is far detuned from the atomic transition line but close to the cavity-mode frequency ω_c .

resonance for bosons or for spinless fermions with contact interactions. Due to the leaking of photons from the cavity, the system should be described by the quantum master equation,

$$\partial_t \rho = -i[H, \rho] + \kappa(2\hat{a}\rho\hat{a}^\dagger - \hat{a}^\dagger\hat{a}\rho - \rho\hat{a}^\dagger\hat{a}), \quad (2)$$

where 2κ is the loss rate of the cavity photons.

If the cavity was directly driven by another pump laser such that the cavity field is a coherent state $\hat{a} \rightarrow \alpha$, then the particles would experience a static effective potential $V_{\text{eff}}(\alpha) = \sum_{j=1}^L [2\lambda \text{Re}(\alpha)u_j + U|\alpha|^2 u_j^2] \hat{c}_j^\dagger \hat{c}_j$. In the case where β is an irrational number and $U = 0$, this reproduces the celebrated Aubry-André model, which exhibits a delocalization-localization transition for all the eigenstates [58]. Even when $U \neq 0$, this transition still survives but now with mobility edges in the energy spectrum [59]. We are interested in cases without this direct drive in which the cavity has its own quantum dynamics and the atoms feel a dynamical potential.

Mean-field steady state. From Eq. (2), one finds that the mean cavity field $\alpha(t) = \langle \hat{a}(t) \rangle$ evolves as

$$i \partial_t \alpha = (\Delta - i\kappa + UR)\alpha + \lambda\Theta, \quad (3)$$

where $\Theta = \sum_j u_j \langle \hat{c}_j^\dagger \hat{c}_j \rangle$ and $R = \sum_j u_j^2 \langle \hat{c}_j^\dagger \hat{c}_j \rangle$. We seek a steady state in which $\partial_t \alpha = 0$ and find $\alpha = -\frac{\lambda\Theta}{\Delta - i\kappa + UR}$. The expectation value of $\langle \hat{c}_j^\dagger \hat{c}_j \rangle$ can be obtained from the ground state of the mean-field Hamiltonian $H_{\text{MF}}(\alpha) = -J \sum_{j=1}^L (\hat{c}_{j+1}^\dagger \hat{c}_j + \text{H.c.}) + V_{\text{eff}}(\alpha)$.

We consider one atom in the cavity and numerically obtain the steady-state phase diagram, see Fig. 2. To describe the localization of the particle, we calculate the inverse participation ratio in real space of the atomic wave-function $p = \sum_{j=1}^L |\langle \hat{c}_j^\dagger \hat{c}_j \rangle|^2$. One notes that highly localized density gives $p \sim 1$; whereas an extended wave function has $p \sim 1/L$.

In the weak pumping regime, the system is in the “normal” phase, which has no superradiance $\alpha = 0$, and the effective potential vanishes $V_{\text{eff}}(\alpha) = 0$. So the atomic states are delocalized. When U is large, as the pumping strength increases, the system undergoes a second-order phase transition from the normal phase to a “delocalized superradiant” phase, see Fig. 2(b). As a result the effective potential $V_{\text{eff}}(\alpha)$ is nonzero, and the atomic density is modulated but still delocalized. For larger pumping strength, the system undergoes a transition into a “localized superradiant” phase. In this phase, the effective potential becomes so large that the atomic wave function is localized. In the small- U regime, these two transitions merge into one first-order transition where the cavity field and the effective

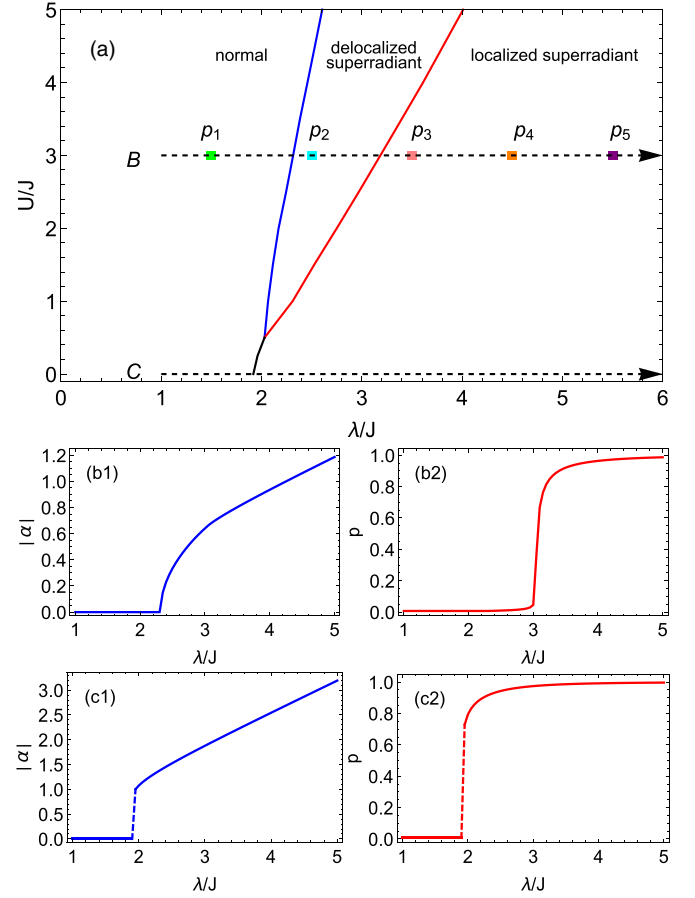


FIG. 2. (a) Phase diagram of the mean-field steady state. (b1) and (b2) Second-order phase transition along line B in (a). (b1) Mean cavity field α . (b2) Inverse participation ratio in real-space p . (c1) and (c2) First-order phase transition along line C in (a). Here $L = 201$, $\beta = (\sqrt{5} - 1)/2$, $\phi = \pi/2$, $\Delta/J = 1$, and $\kappa/J = 1.2$. The square dots p_i ($i = 1, \dots, 5$) represent the pumping strengths $\lambda/J = 1.5, 2.5, 3.5, 4.5, 5.5$, respectively, and $U/J = 3$.

potential suddenly jump to large values [Fig. 2(c)]. Note that these conclusions are also valid for the N boson system with the same phase diagram provided we keep Δ/J , κ/J invariant and scale $\lambda/J \rightarrow \lambda/(JN)$, $U/J \rightarrow U/(JN)$. The appearance of a localized superradiant phase is consistent with a previous study [39].

Wave-packet spreading. For a single atom, there will be no sharp superradiant phase transition as the mean photon occupation will grow continuously with pump strength. However, there will still be a localization-delocalization transition at the mean-field level. It is natural to ask how this is affected by cavity fluctuations. To investigate this issue, we have studied how an atomic wave packet spreads, which would be completely different for localized and delocalized regimes. We set the initial state to be the atom located in the center of the lattice and the cavity empty. We then consider turning on the pump laser and calculate the time evolution of the wave-packet width $\sigma(t) = \sqrt{\langle X^2 \rangle - \langle X \rangle^2}$, where $X = \sum_j j \hat{c}_j^\dagger \hat{c}_j$ is the center of mass of the wave packet. We find, quite generally, that the width grows as a power-law $\sigma(t) \sim t^\nu$ at long times. However, the nature of this growth is a surprisingly subtle

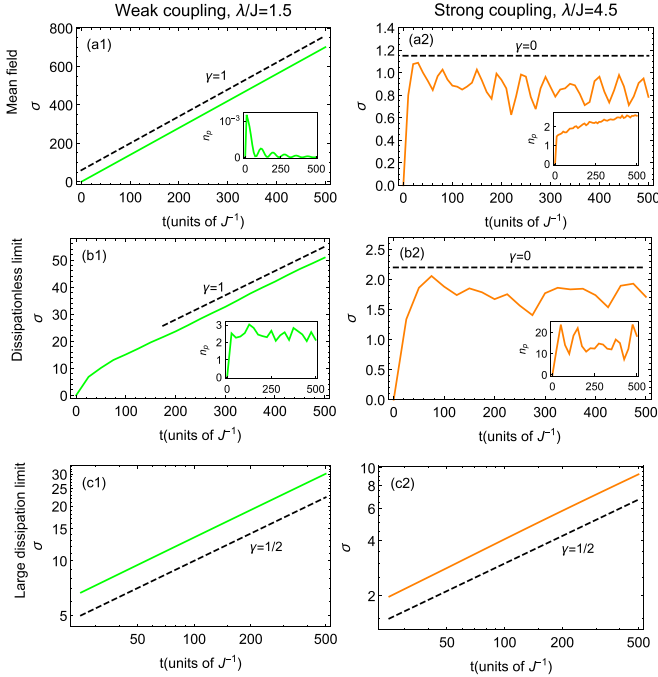


FIG. 3. (a1) and (a2) Time evolution of wave-packet width $\sigma(t)$ and phonon number $n_p(t)$ from the mean-field dynamics. The dashed line is a guide for a ballistic ($\gamma = 1$) or a saturated ($\gamma = 0$) behavior. (b1) and (b2) Dissipationless nonequilibrium dynamics. (c1) and (c2) Dynamics in the large dissipation limit. The dashed line is a guide for diffusion $\gamma = 1/2$. Here $\beta = (\sqrt{5} - 1)/2$, $\phi = \pi/2$, $\Delta/J = 1$, $\kappa/J = 1.2$, and $U = 0$.

issue: Its qualitative form requires an accurate description of the quantum fluctuations of the driven-damped cavity field. We illustrate this by first presenting results of mean-field dynamics and two limiting cases of the cavity damping (for these cases we set $U = 0$ for simplicity).

Mean-field dynamics. At the mean-field level, the cavity field evolves as Eq. (3); whereas the evolution of the atomic wave function is governed by the mean-field Hamiltonian $H_{MF}(\alpha)$. We numerically solve these two coupled nonlinear equations, obtaining the photon number $n_p(t) = |\alpha(t)|^2$ and the wave-packet width $\sigma(t)$, see Figs. 3(a1) and 3(a2). The photon number first rises from zero to a nonzero value in a short time and then slowly approaches a steady-state value. For small pumping strengths, the wave packet spreads ballistically $\gamma = 1$. Whereas for large pumping strength, the width saturates at long times, indicating localized behavior $\gamma = 0$.

Dissipationless limit. We now consider the dissipationless limit $\kappa = 0$. The system is then closed, and the dynamics is given by unitary evolution under the Hamiltonian (1). We numerically simulate the unitary evolution process. The results are shown in Figs. 3(b1) and 3(b2). Note that, except for larger photon number fluctuations, the behavior of the wave-packet spreading is similar to the mean-field results. These qualitative forms of dynamics (both mean field and dissipationless limit) are consistent with the steady-state's phase diagram: the delocalized phase exhibits ballistic transport, whereas transport is absent in the localized phase.

Large dissipation limit. We now consider the opposite limit in which the dissipation κ is so large that the lifetime of

the cavity is negligible. In this case, the cavity field will adiabatically follow the distribution of the atom density with $\hat{a} \approx -\frac{\lambda}{\Delta - i\kappa} \hat{K}$, where $\hat{K} = \sum_j u_j \hat{c}_j^\dagger \hat{c}_j$. Since the cavity field is fixed by the atomic density, one can substitute this formula into the Hamiltonian (1) and the quantum master equation (2) to obtain the effective master equation for the atoms as $\partial_t \rho_a = -i[H_{\text{eff}}, \rho_a] + \kappa'(2\hat{K}\rho_a\hat{K} - \hat{K}^2\rho_a - \rho_a\hat{K}^2)$. Here ρ_a is the reduced density matrix of the atoms, and the effective Hamiltonian is $H_{\text{eff}} = -J \sum_{j=1}^L (\hat{c}_{j+1}^\dagger \hat{c}_j + \text{H.c.}) + V' \sum_{j=1}^L u_j^2 \hat{c}_j^\dagger \hat{c}_j$ with $V' = -\frac{2\lambda^2\Delta}{\Delta^2 + \kappa^2}$ and $\kappa' = \frac{\lambda^2\kappa}{\Delta^2 + \kappa^2}$. This effective model describes an atom hopping in a quasiperiodic lattice with a global noise, which is imposed by the damped cavity field. We have numerically solved this effective quantum master equation. The temporal dynamics of the width of the atomic wave packet is shown in Figs. 3(c1) and 3(c2). We find that, in this large dissipation limit, the wave packet always spreads diffusively $\sigma \sim t^{1/2}$, both where the mean-field solution shows delocalized [Fig. 3(c1)] and localized [Fig. 3(c2)] behaviors. Thus, this global noise destroys the coherence and makes the atom diffuse like a classical Brownian particle at long times.

Quantum trajectory method. After considering mean-field dynamics and these two limiting cases, we now investigate the generic situation in which the cavity dissipation is finite. We employ the so-called quantum trajectory method [60], which is a stochastic way to simulate the quantum master equation by averaging over many quantum trajectories.

We have used this method to simulate the wave-packet spreading for different pumping strengths. The results are plotted in Fig. 4. In Fig. 4(a), one can see a typical dynamics of the system. Similar to the dissipationless limit, the photon number rises to a nonzero value on a short time scale. After that, the cavity field enters into a quasisteady state in which the photon number has small fluctuations around its mean. Note that the fluctuation amplitude is much smaller than that in the dissipationless limit [Fig. 3(b2)] as the existence of the cavity dissipation suppresses these fluctuations. At short times, the width of the wave packet grows quickly from zero since the cavity field has not yet built up a large effective potential. However, at long times, after the cavity field has reached its quasisteady state, we find that the wave packet spreads according to anomalous diffusion $\sigma \sim t^\gamma$ with $0 < \gamma < 1$. We find that the exponent γ depends on the pumping strength and other parameters. As shown in Fig. 4(b), when the pumping strength is small, γ is relatively large, corresponding to superdiffusion $\gamma > 1/2$. When the pumping strength is large, γ becomes relatively small, crossing over to the subdiffusion regime $\gamma < 1/2$ [see Fig. 4(c)]. This behavior is very different from the dissipationless and large dissipation limits as well as mean-field dynamics. This indicates that the observed anomalous diffusion is a result of both the dissipation and the cavity dynamics. At the mean-field level, the atomic wave function has a delocalization-localization transition in the steady state with a sharp change from $\gamma = 1$ (ballistic) to $\gamma = 0$ (localized), see Fig. 4(c). Our results show that a full account of cavity fluctuations and dissipation removes any sharp transition, leaving a crossover characterized by a continuously varying anomalous diffusion exponent. With increasing dissipation we find that this exponent approaches $1/2$, consistent with the adiabatic elimination result.

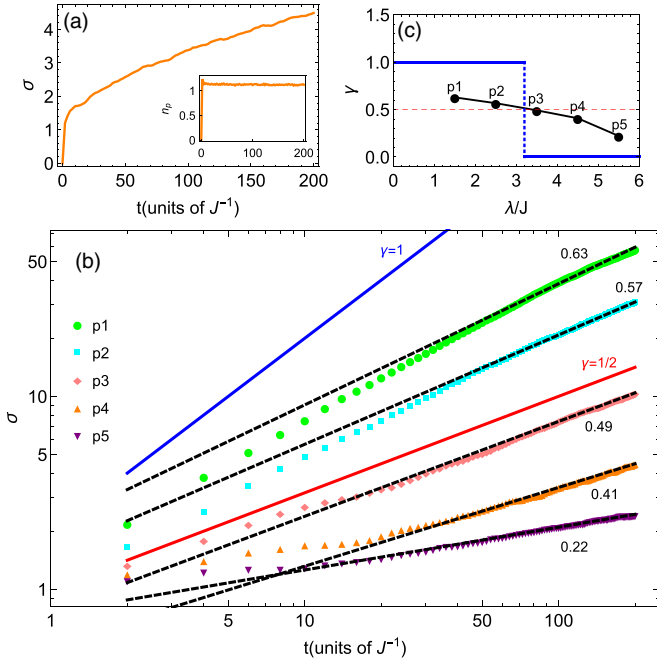


FIG. 4. (a) Wave-packet width and photon number evolution from the exact quantum trajectory method. The parameters are given by the point p_4 in Fig. 2(a). (b) Evolution of the wave-packet width. The dashed lines are the results of fitting to $\sigma = at^\gamma$, and the corresponding numbers are the exponents. The two solid lines represent the ballistic $\gamma = 1$ and diffusive $\gamma = 1/2$ cases. (c) The exponent γ crosses over from superdiffusion to subdiffusion with increasing pump strength. [The parameters of p_i can be found in Fig. 2(a).] For comparison, the solid line is the mean-field result showing a transition from ballistic transport $\gamma = 1$ to localization $\gamma = 0$, whereas the dashed line marks the diffusive value $\gamma = 1/2$.

How can we understand this anomalous diffusion? We plot the evolution of the photon number and the wave-packet width for a single quantum trajectory in Fig. 5. Comparing the photon number and the width, one finds that when the photon number is large the width almost does not grow: At these times, the effective potential induced by the cavity is very strong such that the wave packet is localized and cannot spread freely. When the cavity field fluctuates to a small value, it reduces the effective potential: At these times, the wave packet can spread ballistically until the revival of the photon number. With the help of this picture, we can map the particle hopping into a Lévy walk with rests [52,53]. When the cavity field is lower

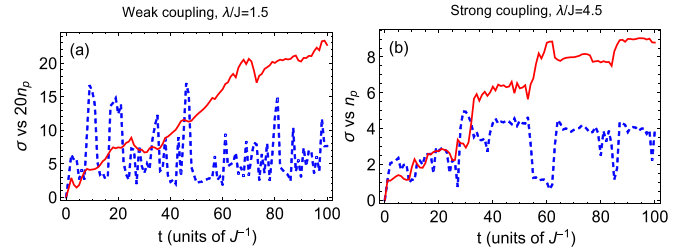


FIG. 5. Individual quantum trajectories of the stochastic evolution in: (a) the superdiffusive regime and (b) the subdiffusive regime. The solid line is the wave-packet width, and the dashed line is the photon number [multiplied by 20 in (a)]. Here $\beta = (\sqrt{5} - 1)/2$, $\phi = \pi/2$, $\Delta/J = 1$, $\kappa/J = 1.2$, and $U = 0$.

than a threshold, the particle moves ballistically at a certain maximal velocity set by the bandwidth. When the cavity field exceeds the threshold due to the Anderson localization the motion is switched off, and the particle is at rest. The time intervals of the “on” and “off,” i.e., moving time and waiting time are random variables since the cavity is affected by the noise from the environment. Crucially, we find that, in the large pumping regime, the distribution of waiting times has a broad tail, leading to subdiffusive behavior. Whereas in the small pumping regime, the broad tail of the moving time distribution dominates and gives superdiffusion. By increasing the pump strength, one increases the mean cavity field and decreases the switching threshold. This gradually tunes the distribution of waiting time and the moving time, resulting in a crossover from subdiffusion to superdiffusion.

Final remarks. Anomalous diffusion is predicted in other quantum systems with specific forms of colored noise [61–65]. In our model anomalous diffusion arises naturally in a very simple experimental setting with a generic form of damping. The wave-packet spreading could be detected by *in situ* imaging. In addition, the anomalous properties could also be detected from the photons leaking from the cavity [28] for which we predict long-tailed distributions of lower and higher cavity occupations. It will be interesting to consider situations in higher dimensions or for larger particle densities in which cavity-mediated interactions will also play a role.

Acknowledgments. This work was supported by EPSRC Grants No. EP/K030094/1 and No. EP/P009565/1. Statement of compliance with EPSRC policy framework on research data: All data accompanying this publication are directly available within the publication.

- [1] H. Ritsch, P. Domokos, F. Brennecke, and T. Esslinger, *Rev. Mod. Phys.* **85**, 553 (2013).
- [2] J. D. Thompson, T. G. Tiecke, N. P. de Leon, J. Feist, A. V. Akimov, M. Gullans, A. S. Zibrov, V. Vuletić, and M. D. Lukin, *Science* **340**, 1202 (2013).
- [3] A. Goban, C.-L. Hung, S.-P. Yu, J. D. Hood, J. A. Muniz, J. H. Lee, M. J. Martin, A. C. McClung, K. S. Choi, D. E. Chang, O. Painter, and H. J. Kimble, *Nat. Commun.* **5**, 3808 (2014).
- [4] K. Baumann, C. Guerlin, F. Brennecke, and T. Esslinger, *Nature (London)* **464**, 1301 (2010).
- [5] R. Mottl, F. Brennecke, K. Baumann, R. Landig, T. Donner, and T. Esslinger, *Science* **336**, 1570 (2012).
- [6] R. Landig, F. Brennecke, R. Mottl, T. Donner, and T. Esslinger, *Nat. Commun.* **6**, 7046 (2015).
- [7] M. R. Bakhtiari, A. Hemmerich, H. Ritsch, and M. Thorwart, *Phys. Rev. Lett.* **114**, 123601 (2015).
- [8] J. Klinder, H. Keßler, M. R. Bakhtiari, M. Thorwart, and A. Hemmerich, *Phys. Rev. Lett.* **115**, 230403 (2015).
- [9] R. Landig, L. Hruby, N. Dogra, M. Landini, R. Mottl, T. Donner, and T. Esslinger, *Nature (London)* **532**, 476 (2016).

- [10] P. Domokos and H. Ritsch, *Phys. Rev. Lett.* **89**, 253003 (2002).
- [11] D. Nagy, G. Kónya, G. Szirmai, and P. Domokos, *Phys. Rev. Lett.* **104**, 130401 (2010).
- [12] M. J. Bhaseen, M. Hohenadler, A. O. Silver, and B. D. Simons, *Phys. Rev. Lett.* **102**, 135301 (2009).
- [13] S. Gopalakrishnan, B. L. Lev, and P. M. Goldbart, *Phys. Rev. A* **82**, 043612 (2010).
- [14] J. Keeling, M. J. Bhaseen, and B. D. Simons, *Phys. Rev. Lett.* **112**, 143002 (2014).
- [15] F. Piazza and P. Strack, *Phys. Rev. Lett.* **112**, 143003 (2014).
- [16] Y. Chen, Z. Yu, and H. Zhai, *Phys. Rev. Lett.* **112**, 143004 (2014).
- [17] Y. Deng, J. Cheng, H. Jing, and S. Yi, *Phys. Rev. Lett.* **112**, 143007 (2014).
- [18] L. Dong, L. Zhou, B. Wu, B. Ramachandran, and H. Pu, *Phys. Rev. A* **89**, 011602 (2014).
- [19] Y. Chen, H. Zhai, and Z. Yu, *Phys. Rev. A* **91**, 021602 (2015).
- [20] J.-S. Pan, X.-J. Liu, W. Zhang, W. Yi, and G.-C. Guo, *Phys. Rev. Lett.* **115**, 045303 (2015).
- [21] G. Szirmai, G. Mazzarella, and L. Salasnich, *Phys. Rev. A* **91**, 023601 (2015).
- [22] C. Kollath, A. Sheikhan, S. Wolff, and F. Brennecke, *Phys. Rev. Lett.* **116**, 060401 (2016).
- [23] Y. Chen, Z. Yu, and H. Zhai, *Phys. Rev. A* **93**, 041601 (2016).
- [24] A. Sheikhan, F. Brennecke, and C. Kollath, *Phys. Rev. A* **93**, 043609 (2016).
- [25] N. Dogra, F. Brennecke, S. D. Huber, and T. Donner, *Phys. Rev. A* **94**, 023632 (2016).
- [26] F. Brennecke, S. Ritter, T. Donner, and T. Esslinger, *Science* **322**, 235 (2008).
- [27] J. Klinder, H. Keßler, M. Wolke, L. Mathey, and A. Hemmerich, *Proc. Natl. Acad. Sci. USA* **112**, 3290 (2015).
- [28] H. Keßler, J. Klinder, B. P. Venkatesh, C. Georges, and A. Hemmerich, [arXiv:1606.08386](https://arxiv.org/abs/1606.08386).
- [29] C. Maschler and H. Ritsch, *Phys. Rev. Lett.* **95**, 260401 (2005).
- [30] J. Keeling, M. J. Bhaseen, and B. D. Simons, *Phys. Rev. Lett.* **105**, 043001 (2010).
- [31] G. Kónya, G. Szirmai, D. Nagy, and P. Domokos, *Phys. Rev. A* **89**, 051601(R) (2014).
- [32] M. Kulkarni, B. Öztop, and H. E. Türeci, *Phys. Rev. Lett.* **111**, 220408 (2013).
- [33] S. Schutz and G. Morigi, *Phys. Rev. Lett.* **113**, 203002 (2014).
- [34] F. Piazza and H. Ritsch, *Phys. Rev. Lett.* **115**, 163601 (2015).
- [35] W. Zheng and N. R. Cooper, *Phys. Rev. Lett.* **117**, 175302 (2016).
- [36] S. Wolff, A. Sheikhan, and C. Kollath, *Phys. Rev. A* **94**, 043609 (2016).
- [37] L. Zhou, H. Pu, K. Zhang, X.-D. Zhao, and W. Zhang, *Phys. Rev. A* **84**, 043606 (2011).
- [38] H. Habibian, A. Winter, S. Paganelli, H. Rieger, and G. Morigi, *Phys. Rev. Lett.* **110**, 075304 (2013).
- [39] K. Rojan, R. Kraus, T. Fogarty, H. Habibian, A. Minguzzi, and G. Morigi, *Phys. Rev. A* **94**, 013839 (2016).
- [40] R. Metzler, E. Barkai, and J. Klafter, *Phys. Rev. Lett.* **82**, 3563 (1999).
- [41] R. Metzler and J. Klafter, *Phys. Rep.* **339**, 1 (2000).
- [42] I. M. Sokolov and J. Klafter, *Chaos* **15**, 026103 (2005).
- [43] F. Piéchon, *Phys. Rev. Lett.* **76**, 4372 (1996).
- [44] S. Roy, I. M. Khaymovich, A. Das, and R. Moessner, [arXiv:1706.05012](https://arxiv.org/abs/1706.05012).
- [45] G. Kopidakis, S. Komineas, S. Flach, and S. Aubry, *Phys. Rev. Lett.* **100**, 084103 (2008).
- [46] A. S. Pikovsky and D. L. Shepelyansky, *Phys. Rev. Lett.* **100**, 094101 (2008).
- [47] N. Cherroret, B. Vermersch, J. C. Garreau, and D. Delande, *Phys. Rev. Lett.* **112**, 170603 (2014).
- [48] K. Agarwal, S. Gopalakrishnan, M. Knap, M. Müller, and E. Demler, *Phys. Rev. Lett.* **114**, 160401 (2015).
- [49] Y. Bar Lev, D. M. Kennes, C. Klöckner, D. R. Reichman, and C. Karrasch, *Europhys. Lett.* **119**, 37003 (2017).
- [50] Y. Sagi, M. Brook, I. Almog, and N. Davidson, *Phys. Rev. Lett.* **108**, 093002 (2012).
- [51] C. D'Errico, M. Moratti, E. Lucioni, L. Tanzi, B. Deissler, M. Inguscio, G. Modugno, M. B. Plenio, and F. Caruso, *New J. Phys.* **15**, 045007 (2013).
- [52] V. Zaburdaev, S. Denisov, and J. Klafter, *Rev. Mod. Phys.* **87**, 483 (2015).
- [53] J. Klafter and I. M. Sokolov, *First Steps in Random Walks* (Oxford University Press, New York, 2011).
- [54] P. Levy, *Bull. la Soc. Math. Fr.* **67**, 1 (1939).
- [55] F. Bardou, J. Bouchaud, A. Aspect, and C. Cohen-Tannoudji, *Lévy Statistics and Laser Cooling* (Cambridge University Press, Cambridge, UK, 2002).
- [56] S. Diehl, W. Yi, A. J. Daley, and P. Zoller, *Phys. Rev. Lett.* **105**, 227001 (2010).
- [57] See Supplemental Material at <http://link.aps.org/supplemental/10.1103/PhysRevA.97.021601> for the details of the experimental setup and the theoretical model.
- [58] S. Aubry and G. André, *Ann. Israel Phys. Soc.* **3**, 133 (1980).
- [59] J. Biddle and S. Das Sarma, *Phys. Rev. Lett.* **104**, 070601 (2010).
- [60] A. J. Daley, *Adv. Phys.* **63**, 77 (2014).
- [61] H. Grabert, P. Schramm, and G.-L. Ingold, *Phys. Rev. Lett.* **58**, 1285 (1987).
- [62] G. W. Ford and R. F. O'Connell, *Phys. Rev. A* **73**, 032103 (2006).
- [63] N. V. Prokof'ev and P. C. E. Stamp, *Phys. Rev. A* **74**, 020102(R) (2006).
- [64] E. Gholami and Z. M. Lashkemi, *Phys. Rev. E* **95**, 022216 (2017).
- [65] S. Gopalakrishnan, K. R. Islam, and M. Knap, *Phys. Rev. Lett.* **119**, 046601 (2017).